Preprints (www.preprints.org) | NOT PEER-REVIEWED | Posted: 29 January 2021 doi:10.20944/preprints202101.0607.v1

Characterization of As-Prepared (PMMA-PVA)/CuO-NPs Hybrid Nanocomposite Thin Films

A. M. Alsaad[a*], A. A. Ahmad[a], A-R. El-Ali[b], I. A. Qattan, Shatha A. Al Fawares[b], Qais M. Al-Bataineh[a]

[a]*Department of Physical Sciences, Jordan University of Science & Technology, P.O. Box 3030, Irbid-22110, Jordan.*

[b]*Department of Physics, Yarmouk University, 21163 Irbid, Jordan*

[c] *Department of Physics, Khalifa University of Science and Technology, P.O. Box 127788, Abu Dhabi, UAE.*

**Correspondence e-mails: alsaad11@just.edu.jo; amalsaad@unomaha.edu*

Abstract

We report the synthesis and characterization of Poly Methyl-Meth-Acrylate (PMMA)/Poly vinylalcohol (PVA) polymeric blend doped with different concentrations of Copper oxide (CuO) nanoparticles (NPs). The (PMMA-PVA)/CuO nanocomposite hybrid thin films (wt. % = 0%, 2%, 4%, 8%, and 16%) of CuO NPs are deposited on glass substrates via dip-coating technique. The transmittance (T%), reflectance (R%), the absorption coefficient (α), the optical constants [refractive index (*n*), extinction coefficient (*k*)], optical dielectric functions [ε',ε''] are investigated and interpreted. Tauc, Urbach, Spitzer-Fan, and Drude models are employed to calculate the optical bandgap energy (*Eg*) and the optoelectronic parameters of the nanocomposite thin films. The refractive index and optical bandgap energy of of (PMMA-PVA) polymeric thin film are found to be (1.5 to 1.85) and 4.101 eV, respectively. Incorporation of specific concentrations of CuO-NPs in (PMMA-PVA) polymeric thin films leads to a noticeable decrease in the optical bandgap energy and to an increase of the refractive index. Moreover, Fourier Transform Infrared Spectroscopy (FTIR) transmittance spectra are measured and analyzed for undoped and doped polymeric thin films to pinpoint the major vibrational modes in the spectral range (500 and 4000 cm^{-1}), as well as, the nature of network bonding in both systems. Thermal stability of thin films is investigated by performing thermogravimetric analysis (TGA). The TGA thermograms confirm that both doped polymeric thin films are thermally stable at temperatures below 110°C which enables them to be attractive for a wide range of optical and optoelectronic applications. Our results indicate that optical, vibrational and thermal properties of both polymeric thin films can be tuned for specific applications by appropriate corporation of particular concentrations of CuO-NPs.

Keywords: Organic-Inorganic Blends; Poly Methyl-Meth-Acrylate (PMMA); Poly-vinyl-alcohol (PVA); Copper oxide nanoparticles (CuONPs); Optical Characterization; Thermal stability; Surface Morphology.

© 2021 by the author(s). Distributed under a Creative Commons CC BY license.

Preprints (www.preprints.org) | NOT PEER-REVIEWED | Posted: 29 January 2021 doi:10.20944/preprints202101.0607.v1

1. Introduction

Organic-Inorganic hybrid nanocomposite thin films are of prime importance. This class of smart functional materials exhibit outstanding physical, chemical, thermal and optical properties and thus plays a major role in the fabrication of modern scaled devices. Combining metal nanoparticles and polymers enhances the optical properties and alters the mechanical behavior of the polymer composite [1]. Employing a high refractive index material in optical applications frequently requires higher optical transparencies [1-4]. Polymers with high refractive index have fascinated several research groups due to their potential applications in cutting-edge optoelectronic devices such as organic light emitting diode devices [5], high performance substrates for advanced display devices [6], antireflective coatings for advanced optical applications [7] and micro lens components for charge coupled devices or complementary metal oxide semiconductor [8]. Poly Vinyl-Alcohol (PVA) has been applied in the industrial, commercial, medical, and food sectors. It has been used to produce surgical threads, paper products, and food packaging materials. PVA has attracted considerable attention due to its attractive film-forming, good processability, biocompatibility, and good chemical resistance. It is a solubilized crystalline structure which is easily degradable in water [9, 10]. This polymer is widely used for blending with other polymer compounds such as, biopolymers and other polymers with hydrophilic properties. Owing to the enhanced structure, mechanical, and hydrophilic properties, the polymerized thin films can be utilized for various industrial applications. The addition of an inorganic material to the polymeric matrix is advantageous to further enhance the chemical, structural and physical properties [9]. PVA has OH groups arranged regularly from one side of the plane to the other, thus providing interchain hydrogen bond networks. This may induce high optical clarity and polarization response in the resulting hybrid polymerized thin films. Consequently, PVA polymer can be utilized in photovoltaic and optoelectronic devices [1]. Furthermore, Poly Methyl-Methacrylate (PMMA) can withstand temperatures between 70 up to 100°C. Also, it possesses very good optical properties with refractive index ranging between 1.3 and 1.7 [4]. Owing to its high impact strength, lightweight, and shatter resistance, the PMMA is one of the best organic optical materials and it is widely used as a substitute for inorganic glass [11]. The PMMA polymer is selected for this study owing to several properties such as, its safety, chemical inertness, very good electrical properties, and excellent thermal stability. Additionally, it has been reported to be suitable for numerous imaging and non-imaging microelectronics, sensors, and conductive devices [12]. Copper Oxide nanoparticles (CuO-NPs) are black solid inorganic particles. CuO-NPs exhibit a bandgap energy of 1.2 eV and adopts p-type conductivity due to the excess of oxygen or copper vacancies in its structure [13]. We have selected CuO-NPs in this study based on its unique properties such as low cost, non-toxicity, ability to diffuse easily in polymers, good electronic and thermal properties, chemical stability, high dielectric constant of 18.1, and a refractive index of 1.4 [13]. CuO-NPs compounds have been technologically implemented in photothermal and solar energy materials

Preprints (www.preprints.org) | NOT PEER-REVIEWED | Posted: 29 January 2021 doi:10.20944/preprints202101.0607.v1

[13], supercapacitor [14], gas sensors and batteries [15], and optoelectronic devices. Dip coating technique is utilized to synthesize (PMMA-PVA)/CuO NPs polymeric nanocomposite thin films. UV-Vis spectrometry measurements is performed, as well as, employing a combination of classical optical models are exploited to measure, analyze and interpret transmittance (T %), reflectance (R %), index of refraction (n), extinction coefficient (k), Urbach energy (E_U) and optical bandgap energy (E_g). Chemical and thermal properties of (PMMA-PVA)/CuO NPs nanocomposite thin films are investigated using FTIR and TGA techniques.

2. Experimental Details

2.1 Preparation of Copper oxide Nanoparticles (CuO-NPs)

CuO-NPs are prepared by using the hydrothermal method. We mix 2g of Copper (II) nitrate trihydrate [$CuH_2N_2O_7$] with 0.5g of hexamethylenetetramine (HMT) [$(CH_2).6N_4$] in a (beaker A). The contents of beaker A were dissolved in 50 ml of distilled water with a pH = 8. The solution is then placed in hot path at 90 $°C$ for 5 h to obtain powdered CuO-NPs. The obtained CuO-NPs were washed three times with distilled water to remove impurities and residuals [9], centrifuged and heated at temperatures ranging from 60 to 70 °C for 24 h. Finally, having obtained CuO-NPs in the powder form, they were then placed in the furnace at a temperature of 400 $°C$ for 2 h [16].

2.2 Synthesis of (PMMA-PVA) doped by CuO-NPs Thin Films

The glass substrates are cleaned with warm tap–water then rinsed with ionized acidic water of (pH = 3.5) to remove the surface oxidized layer and greases and then dipped in acetone. The substrates are then bathed in the ultrasonic path of distilled water for five minutes and dried with cold air. 1 g of PMMA and 1 g of PVA are dissolved separately in 200 ml of Chloroform [$CHCl_3$]. (PMMA-PVA) solution is obtained by mixing (PMMA and PVA) solutions in a 1:1 volume ratio using a magnetic stirrer for 24 h to enhance the homogeneity. PMMA-PVA solution is then filtered using 0.45 µm Millipore filter before dip coating on the glass substrates. The films are synthesized at room temperature of 27oC under atmospheric pressure [19]. The PVA polymers prevent the aggregation of the CuO-NPs by the organic surface modification and keep the CuO-NPs dispersed in PVA matrix at the nano scale. The final solutions are filtered by paper-filter (0.45 µm in dimension). The viscosity of sol-gel solutions ranges between 1.2079 and 2.8935 Cp. The (PMMA-PVA)/CuO nanocomposite solutions are deposited as a thin layer on glass substrate using dip-coating technique for 2 h forming nanocomposite thin films

Preprints (www.preprints.org) | NOT PEER-REVIEWED | Posted: 29 January 2021 doi:10.20944/preprints202101.0607.v1

with average thickness of 500 nm with a maximum standard deviation of 7.5%. The thickness of thin films is confirmed by Scanning Electron Spectroscopy (SEM). The nanocomposite thin films are obtained by allowing the solvent to evaporate for 15 min at 700C to evaporate the solvent and organic residues. The withdrawal speed ranged from 10-80 cm min- 1. The multilayers of (PMMA-PVA)/ CuO nanocomposites thin films are then analysed and interpreted interpreted [17].

3. Results and Discussion

3.1 UV-Vis Spectroscopy

We employ a UV–Vis spectrophotometer to investigate the optical properties of the (PMMA-PVA)/CuO nanocomposite thin films containing various concentrations of CuO-NPs. Particularly, we investigate the spectral behavior of transmittance ($T\%$) and reflectance ($R\%$). Optical constants such as absorption coefficient (α), optical bandgap energy (E_g), Urbach energy (E_U), optical constants (n and k), and optical dielectric functions (ε_1 and ε_2) are measured, analyzed and interpreted. Moreover, using TGA analysis, we investigate the thermal stability. In addition, FTIR analysis is conducted to investigate the bonding and the vibrational bands of the (PMMA-PVA)/CuO films. The FTIR results reveal some sorts of interaction between the constituents of (PMMA-PVA)/CuO nanocomposite thin films as indicated by the induced changes in the vibration modes and the band position.

Figure 1 shows the transmittance spectra of (PMMA-PVA)/CuO nanocomposite thin films as a function of the wavelength of incident light. The figure clearly shows a sort of ion transfer mechanism between (PMMA-PVA) polymer composite and CuO-NPs. The transmittance values of undoped (PMMA-PVA) polymeric thin film in the visible region (visible region, $\lambda \geq$350 nm) is found to be about 91.6%. This behavior indicates an excellent excitation leads to a sharp electron transition from the valence band to the conduction band. Interestingly, the effect of introducing CuO-NPs contents in (PMMA-PVA) polymeric thin films leads to a decrease in transmittance values in the visible region, this change is found to be gradual and nonlinear. Our results indicate that (PMMA-PVA)/CuO nanocomposite thin films with (wt.% = 2% and 4%) of CuO-NPs exhibit transmittance values of 77% and 72% at λ = 550 nm, respectively. Moreover, increasing the concentration of CuO-NPs to (wt.% =

Preprints (www.preprints.org) | NOT PEER-REVIEWED | Posted: 29 January 2021 doi:10.20944/preprints202101.0607.v1

8% and 16%) leads to a decrease in the transmittance to 68% and 65% at λ = 550 nm, respectively. The loss of transparency is attributed to scattering by NPs within the organic polymers [18]. This occurs when the particle size is smaller than the wavelength or it could happen as a result of electron transitions between polymer components and Cu^{+} ions of the CuO-NPs [19]. Figure 2 shows the reflectance spectra of (PMMA-PVA)/CuO nanocomposite thin films for various CuO-NPs contents as a function of the wavelength of incident light. At $\lambda \geq$350 nm, reflectance values slightly decrease as the wavelength is increased. The reflectance of undoped (PMMA-PVA) polymeric thin film is found to be about 4.9% at $\lambda =$ 550 nm. Introducing (wt. % = 2%, 4%, 8%, and 16%) of CuO-NPs in (PMMA-PVA) polymeric thin films leads to an increase of the reflectance to 6.5% in the visible region. The average sum of the transmittance and the reflectance of (PMMA-PVA)/CuO nanocomposite thin films is found to be less than one. This indicates the possibility of scattering or absorption of the incident light from constituents of (PMMA-PVA)/CuO nanocomposite thin films [20].

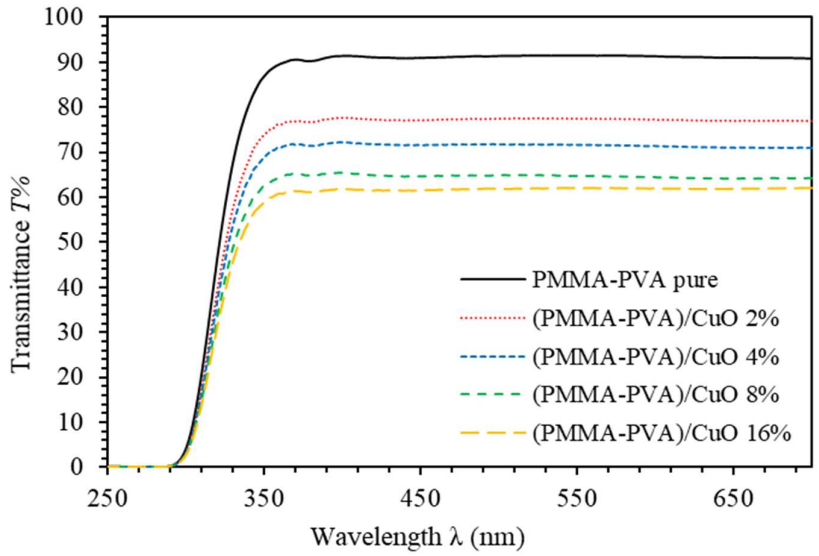

Figure 1. Transmittance spectra of (PMMA-PVA)/CuO nanocomposite thin films as a function of wavelength for various CuO NPs concentrations.

Preprints (www.preprints.org) | NOT PEER-REVIEWED | Posted: 29 January 2021 doi:10.20944/preprints202101.0607.v1

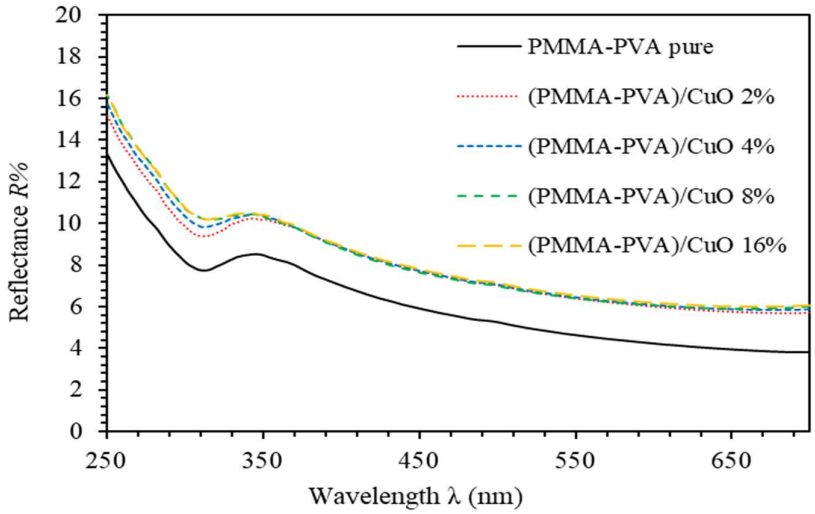

Figure 2. Reflectance spectra of (PMMA-PVA)/CuO nanocomposite thin films as a function of wavelength for various CuO-NPs concentrations.

Figure 3 shows the absorbance coefficient (α) of (PMMA-PVA)/CuO nanocomposite thin films as a function of the wavelength of incident light. Obviously, all (PMMA-PVA)/CuO nanocomposite thin films exhibit very small values of α in the visible region. However, α attains higher values in the UV region ($\lambda \leq 350\ nm$). Furthermore, introducing CuO-NPs contents in (PMMA-PVA) polymeric thin films leads to an increase of α values. The increase in α values maybe attributed to the significant decrease in the inter-band transitions [18]. The (PMMA-PVA)/CuO nanocomposite thin films have strong absorption in the UV region and a strong transition in the visible region. Thin films of such features may act as key candidate potential materials for optoelectronic devices operating in the UV spectral region and can be employed as solar cell absorber or optical windows [18, 21].

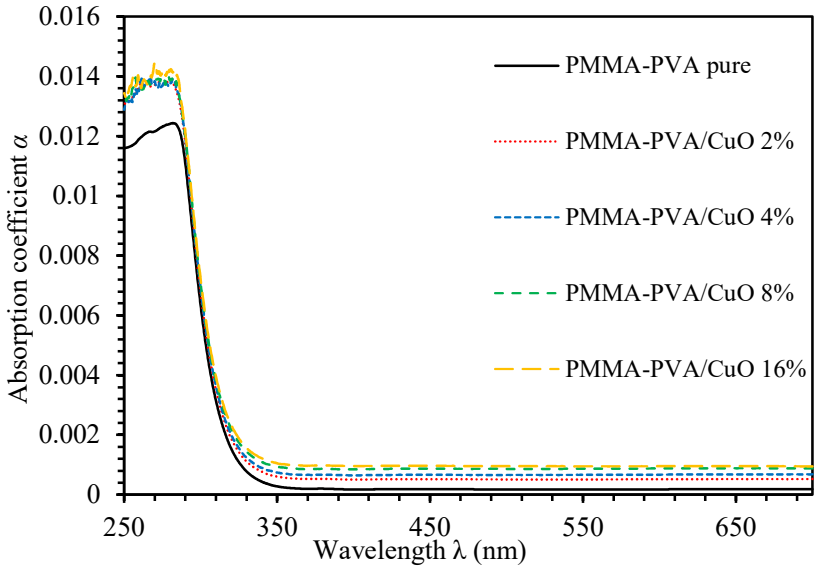

Figure 3. Absorbance coefficient spectra of (PMMA-PVA)/CuO nanocomposite thin films as a function of wavelength for various CuO-NPs concentrations.

Figure 4. shows the refractive index (n) spectra of (PMMA-PVA)/CuO nanocomposite thin films for various CuO-NPs contents as a function of wavelength. For the spectral region ($\lambda <$

Preprints (www.preprints.org) | NOT PEER-REVIEWED | Posted: 29 January 2021 doi:10.20944/preprints202101.0607.v1

$350\ nm$), incident light frequency exactly matched with the plasma frequency [18]. For $\lambda \geq 350\ nm$, n decreases slightly as the wavelength is increased. Our results indicate that n of undoped (PMMA-PVA) polymeric thin film lies in the range (1.5-1.85), as the wavelength is decreased. Introducing wt. % of (2%, 4%, 8% and 16%) of CuO-NPs into (PMMA-PVA) polymeric thin films leads to an increase of n to 1.68 at $\lambda = 550$ nm. This change is independent of the concentration level of CuO-NPs incorporated in (PMMA-PVA) polymeric thin films. This increase in n value of (PMMA-PVA)/CuO nanocomposite thin films could be attributed to the condensation of smaller nanoparticles into larger clusters due to the insertion of NPs [22]. The constant value of ($n = c/v$), irrespective of the CuO-NPs doping level, indicates that photons propagate through the constituents of (PMMA-PVA)/CuO nanocomposite thin films uniformly [20]. Moreover, n is closely related to the reflectance as demonstrated by equation (2.8). Consequently, reflectance is found to be independent of the doping level of the CuO-NPs. The obtained fixed high values of n of (PMMA-PVA)/CuO nanocomposite thin films have a direct implication, as they can be employed in opto-electronic applications such as, optical waveguides, filters, lenses, anti-reflective coatings, and photonic device applications (solar cells and encapsulation materials for light emitting diodes (LEDs)) [1-3, 5, 18, 22-24].

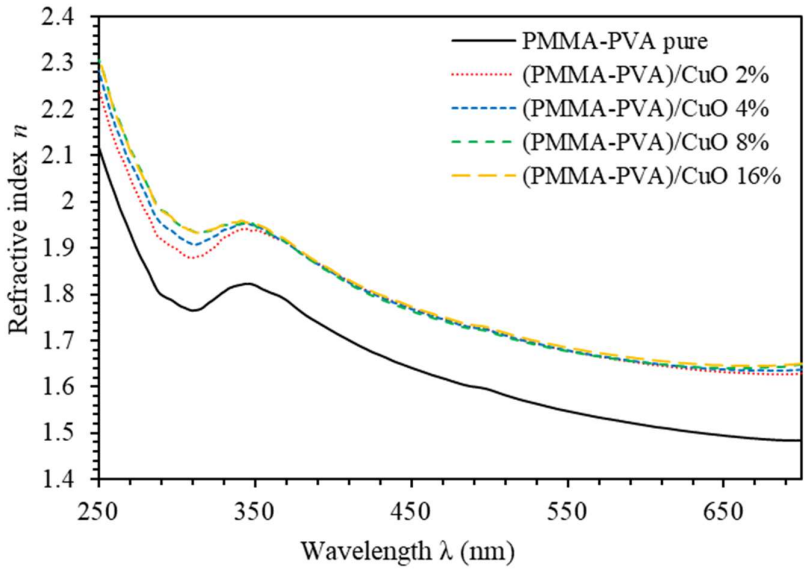

Figure 4. Reflectance index spectra of (PMMA-PVA)/CuO nanocomposite thin films as a function of wavelength for various CuO-NPs concentrations.

Extinction coefficient (k) measures the absorption loss. Specifically, It measures the fraction of light lost by scattering and absorption per unit distance of the medium [25]. It can be expressed as, $k = \alpha\lambda/\ 4\pi$ [25]. Figure 3.5 shows k spectra of (PMMA-PVA)/CuO nanocomposite thin films as a function of the wavelength for various CuO-NPs concentrations. Clearly, k exhibits high values in the UV region and small values in the visible region. At $\lambda = 550$ nm, k increases to 0.0081, 0.0291, 0.0381, 0.0416, and 0.0417, respectively, as (wt. % = 0%, 2%, 4%, 8%, and 16%) of CuO-NPs is added to (PMMA-PVA) polymeric thin films. The k parameter is directly proportional to α as indicated by equation (2.6) [19]. Therefore, such behavior of k indicates the presence of light absorption by (PMMA-PVA)/CuO nanocomposite thin films in the UV spectral region, as well as, incident light lost due to scattering in the visible light region [1]. Our results indicate that (PMMA-PVA)/CuO nanocomposite thin films exhibit excellent loss of optical transparency in visible spectral region [2].

Preprints (www.preprints.org) | NOT PEER-REVIEWED | Posted: 29 January 2021 doi:10.20944/preprints202101.0607.v1

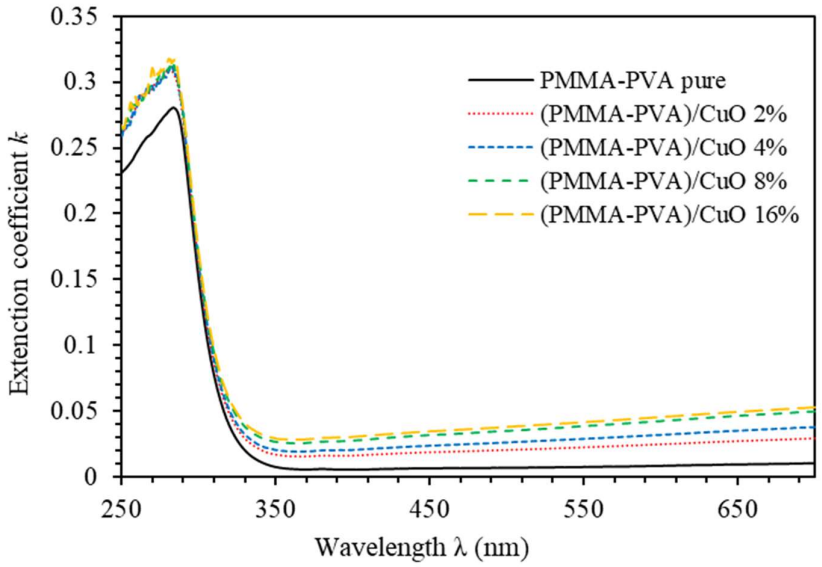

Figure 3.5. Extinction coefficient spectra of (PMMA-PVA)/CuO nanocomposite thin films as a function of wavelength for various CuO-NPs concentrations.

The optical dielectric constant (ε′) indicates the suppression of the speed of light in the medium [26]. The complex dielectric function is $\varepsilon = \varepsilon' + i\varepsilon''$, where ε' is given by, $\varepsilon' = n^2 + k^2$. The imaginary part is called optical dielectric loss (ε'') and given by, $\varepsilon'' = 2nk$ [27]. Figure 3.6 shows ε' spectra of (PMMA-PVA)/CuO nanocomposite thin films as function of wavelength for various CuO-NPs concentrations. The value of ε' of undoped (PMMA-PVA) thin film lies in the range (2.2-3.3). Insertion of (wt. % = 2%, 4%, 8%, and 16%) of CuO-NPs into (PMMA-PVA) results in an increase of ε' to about 2.4 at λ= 550 nm. Remarkably, ε' of (PMMA-PVA)/CuO nanocomposite thin films demonstrates a uniform incremental increase, as CuO-NPs contents in (PMMA-PVA) polymeric thin films are increased [1, 20]. This trend may be attributed to the slight rotation of thermally activated dipoles [28]. The higher dielectric constants due to relatively large polarizability of nonpolar bonds such as C–H, C–C, and C=O [29]. In this work, FTIR spectra measurements of thin films also supports the presence of C–H and C=O bonds [1]. Figure 3.7 shows the optical dielectric loss (ε'') spectra of (PMMA-PVA)/CuO nanocomposite thin films as a function of the wavelength for various CuO-NPs concentrations. Clearly, all as-grown thin films exhibit high ε'' in the UV region. However, the (PMMA-PVA)/CuO nanocomposite thin films exhibit small values of ε'' in the visible region. Therefore, less dissipation of energy from the electric field due to molecular dipoles motion in the visible region is observed [28]. Our results indicate that, at $\lambda = 550$ nm, optical dielectric loss exhibits values of 0.0076, 0.02915, 0.02916, 0.0416, and 0.0417, respectively, as (wt. % = 0%, 2%, 4%, 8%, and 16%) of CuO-NPs is added in (PMMA-PVA) matrix. Remarkably, ($\varepsilon' \gg \varepsilon''$) indicating that (PMMA-PVA)/CuO NPs nanocomposites demonstrate extremely small dissipation of energy and higher speed of propagation of light.

Preprints (www.preprints.org) | NOT PEER-REVIEWED | Posted: 29 January 2021 doi:10.20944/preprints202101.0607.v1

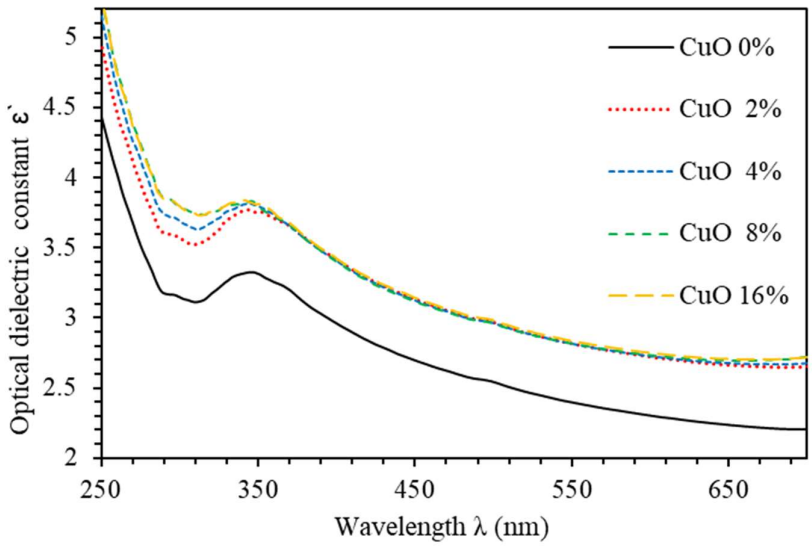

Figure 3.6. Optical dielectric constant (ε′) spectra of (PMMA-PVA)/CuO nanocomposite thin films as a function of wavelength for various CuO-NPs concentrations.

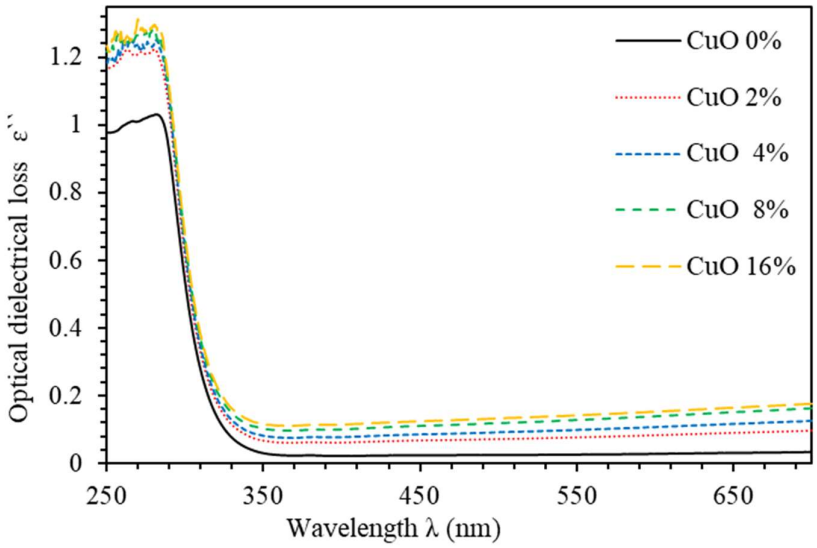

Figure 3.7. Optical dielectric loss (ε″) spectra of (PMMA-PVA)/CuO nanocomposite thin films as function of wavelength for various CuO-NPs concentrations.

Preprints (www.preprints.org) | NOT PEER-REVIEWED | Posted: 29 January 2021 doi:10.20944/preprints202101.0607.v1

Table 1. Refractive index (n), extinction coefficient (k), dielectric permittivity (ε′), and dielectric loss (ε″) of PMMA-PVA-CuO NPs thin films for different concentrations of CuO NPs at $\boldsymbol{\lambda}$ = 500 nm.

(PMMA-PVA)/CuO NPs thin films (wt. %)	Wavelength $\lambda(nm)$	Refractive index n	Extinction constant k	Dielectric permittivity ε'	Dielectric loss ε''
0	550	1.5479	0.0077	2.3960	0.0238
2%	550	1.6776	0.0224	2.8140	0.0752
4%	550	1.6785	0.0291	2.8166	0.0977
8%	550	1.6779	0.0381	2.8137	0.1278
16%	550	1.6845	0.0417	2.8359	0.1404

Tauc plot is based on relating the absorption coefficient with the incident photon energy ($h\upsilon$) as $(\alpha h\upsilon)^2 = \beta(h\upsilon - E_g)$ [30], where β is constant called band tailing parameter, E_g is the band gap energy. It is obtained by plotting ($h\upsilon$) in eV versus $(\alpha h\upsilon)^2$. Figure 8 shows Figure 3.23 shows the Tauc plot of the as-grown doped polymerized thin films. As shown, the optical bandgap energy (E_g) values are obtained by extrapolating the linear part of the relation to the incident photon energy at which E_g equals to the incident photon energy ($h\upsilon$). The E_g of undoped (PMMA-PVA) polymeric thin film is found to be 4.101 eV. As 2% and 4% of CuO-NPs are introduced into (PMMA-PVA) matrix, the value of E_g decreases slightly to 4.0945 eV and 4.0853 eV, respectively. Injection of 8% and 16% of CuO-NPs, into (PMMA-PVA)/CuO nanocomposite thin films lead to a further slight decrease of E_g to 4.0593 eV and 4.0374 eV, respectively. This may be attributed to the ability of CuO-NPs to enhance the ion transfer between the constituents of (PMMA-PVA)/CuO nanocomposite thin films. Furthermore, some sub-bands are generated due to the formation of defect levels leading to facilitate the overpass of electrons from VBM to the CBM [20, 31]. The increase in carriers density in localized states leads to a significant decrease in the transition probabilities of the extended states. As a result, an additional absorption and reduction in the bandgap energy is observed [31].

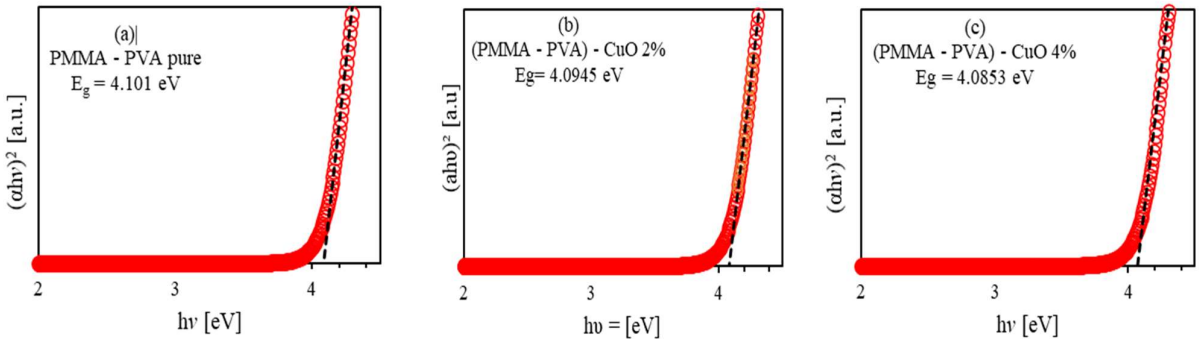

Preprints (www.preprints.org) | NOT PEER-REVIEWED | Posted: 29 January 2021 doi:10.20944/preprints202101.0607.v1

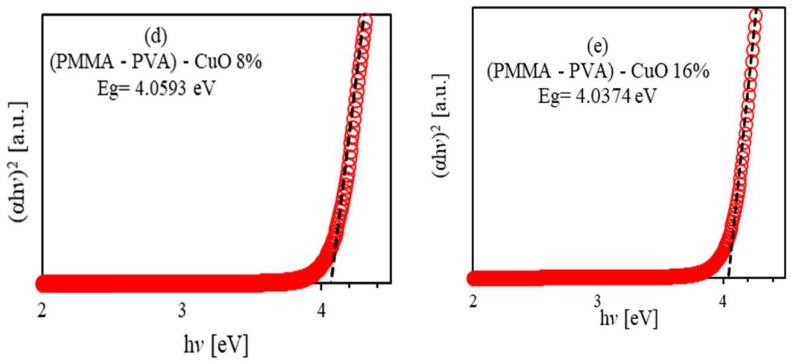

Figure 8. Tauc optical bandgap energy of (PMMA-PVA)/CuO nanocomposite thin films as a function of wavelength for various CuO-NPs concentrations deposited by dip coating Technique.

Urbach's energy E_U is associated with the structural disorder in low-crystalline materials. It is related to the local states broadened into the band gap predominantly due to the occurrence of defects, impurities, and non-crystallinity. The relation between E_U and the absorption coefficient α, and $h\nu$, is given by $\alpha = \alpha_0 \exp(h\nu/E_U)$, where α_0 is a constant [32, 33]. E_U is calculated by plotting lnα vs $h\nu$. The reciprocal of the slopes of the linear portion, below the optical band gap, gives the value of E_U [34]. Figure 9 shows the variation of Urbach energy (E_U) of (PMMA-PVA)/CuO nanocomposites as a function of CuO-NPs. E_U of undoped (PMMA-PVA) film is found to be 190.7 meV. Insertion of (wt. % = 2%, 4%, 8% and 16%) of CuO-NPs increases E_U to 211.1 meV, 224.8 meV, 242.5 meV, and 244.8 meV, respectively. In addition, Urbach energy tail is closely related to the disorder in the film network. The increase in the values of Urbach energy with increasing CuO-NPs contents in (PMMA-PVA)/CuO nanocomposites affirms the existence of defects and impurities [18].

Figure 10 shows the relation between E_g and E_U of (PMMA-PVA)/CuO films for various CuO-NPs concentrations. Clearly, E_U and the band edges of the (PMMA-PVA)/CuO films exhibit a reverse trend. It can be easily noticed that the lowering of bandgap in (PMMA-PVA)/CuO nanocomposite thin films is due to the presence of localized defect states in the bandgap energy near the conduction band minimum and valence band maximum [18, 31]. The decrease of E_U reveals alterations in the structure since Urbach tail parameter is a function of structural disorder [1, 35].

Preprints (www.preprints.org) | NOT PEER-REVIEWED | Posted: 29 January 2021 doi:10.20944/preprints202101.0607.v1

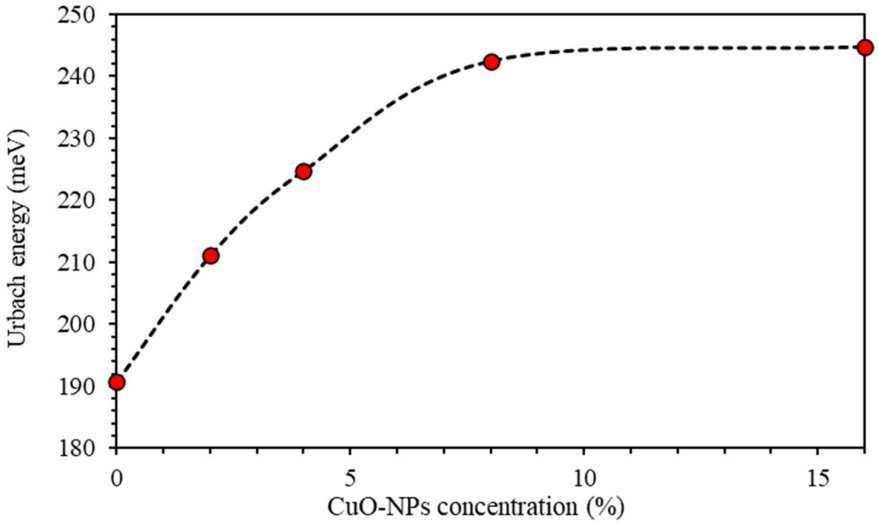

Figure 9. Urbach energy versus the concentration of (PMMA-PVA)/CuO nanocomposites thin films.

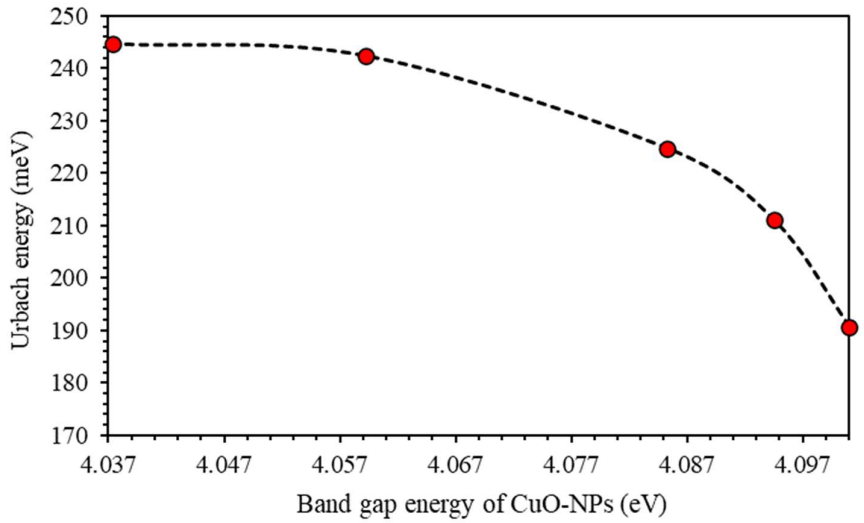

Figure 10. Relationship between the optical energy gap and the Urbach energy of (PMMA-PVA)/CuO nanocomposites thin films.

3.2 Optoelectronic Parameters

The frequency zone investigated determines the contribution of electronic, ionic, dipolar and space charge polarization to the dielectric function. The influence of the space charge contribution is strongly dominant and basically responsible for normal dispersion in the low-frequency region. as proposed by Spitzer-Fan, refractive index $n = \varepsilon'$ and can be related to the density of states (ratio of free carrier to the effective mass, N/m^*) and the high-frequency dielectric constant ε_∞ [36, 37],

$$n^2 = \varepsilon' = \varepsilon_\infty - \frac{1}{4\pi^2\varepsilon_0}\left(\frac{e^2}{c^2}\right)\left(\frac{N_c}{m^*}\right)\lambda^2 \quad (1)$$

Preprints (www.preprints.org) | NOT PEER-REVIEWED | Posted: 29 January 2021 doi:10.20944/preprints202101.0607.v1

where m^* is the effective mass of each carrier. The ε_∞ parameter can be determined from the extrapolation of the linear part of to $\lambda^2 = 0$ as demonstrated by figure 11 illustrating ($n^2 = \varepsilon'$) as a function of λ^2 for (PMMA-PVA)/CuO nanocomposites for various CuO-NPs concentrations. The estimated values of both ε_∞ and N_c/m^* are listed in Table 1. The value of ε_∞ of (PMMA-PVA) films is found to be 2.623 increases to 3.003 as the concentration of CuO-NPs in (PMMA-PVA)/CuO nanocomposite is increased to 16%. The value of ε_∞ is larger than n confirming the existence of the free charge carriers in (PMMA-PVA)/CuO nanocomposites [28, 38].

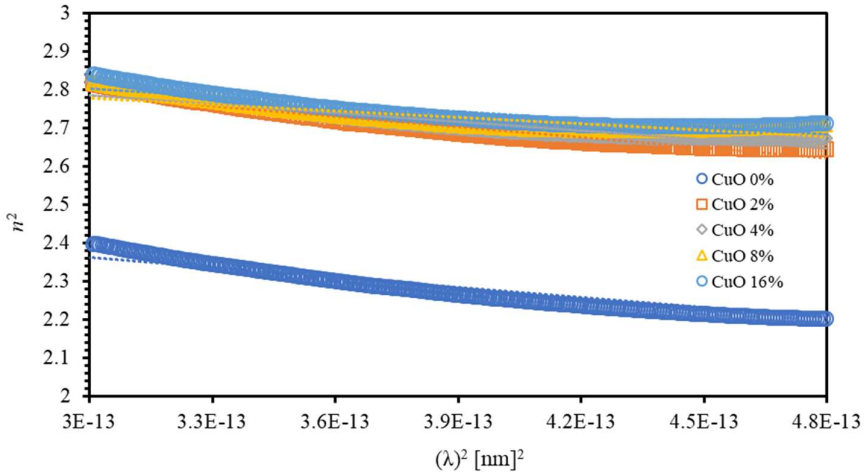

Figure 11. The variation of the real part of the dielectric constant ($n^2 = \varepsilon'$) with the square of the photon wavelength (λ^2) for (PMMA-PVA)/CuO nanocomposites.

Moreover, we investigate the relationship between (ε'') and λ. The relaxation time (τ), optical mobility (μ_{opt}), and optical resistivity (ρ_{opt}) can all be obtained from this relation as formulated by Drude free electron model [36],

$$\varepsilon'' = \frac{1}{4\pi^3\epsilon_0}\left(\frac{e^2}{c^3}\right)\left(\frac{N_c}{m^*}\right)\left(\frac{1}{\tau}\right)\lambda^3 \tag{2}$$

Figure 12 shows the variation of ε'' with λ^3 for the (PMMA-PVA)/CuO nanocomposites for various CuO NPs concentrations. τ can be evaluated from the slope of the plot of ε'' versus λ^3 and from the value of N_c/m^* and taking $m^* = 0.44m_e$ [39]. The μ_{opt} and ρ_{opt} of the films can be expressed as [36],

$$\mu_{opt} = \frac{e\tau}{m^*} \tag{3}$$

$$\rho_{opt} = \frac{1}{e\mu_{opt}N_c} \tag{4}$$

The calculated values of both parameters are presented in Table 1.

Preprints (www.preprints.org) | NOT PEER-REVIEWED | Posted: 29 January 2021 doi:10.20944/preprints202101.0607.v1

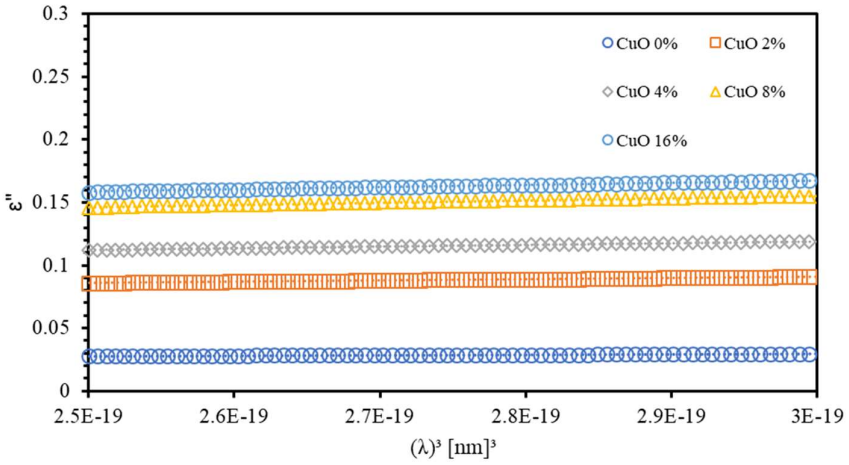

Figure 12. The variation of the spectra of the imaginary part (ε") of (PMMA-PVA)/CuO nanocomposite thin films as a function of (λ^3) for various CuO NPs concentrations.

Table 2. Estimation of some essential optical parameters of (PMMA-PVA)/CuO nanocomposite thin films for various CuO NPs concentrations.

Parameter	CuO 0%	CuO 2%	CuO 4%	CuO 8%	CuO 16%
Density of states, $N_c/m^* * 10^{+57}$ $(m^{-3}.Kg^{-1})$	1.066	1.116	0.944	0.691	0.812
Charge carrier density, $N_c * 10^{+27}$ (m^{-3})	4.273	4.472	3.782	2.770	3.255
High-frequency dielectric constant, ε_∞	2.623	3.058	3.017	2.948	3.003
Relaxation time, $\tau * 10^{-14}$ (s)	2.493	0.987	0.599	0.342	0.402
Optical mobility, $\mu_{opt} * 10^{-3}$	9.951	3.938	2.391	1.364	1.603
Optical resistivity, $\rho_{opt} * 10^{-6}$	1.470	3.548	6.910	16.548	11.979

3.3 Fourier Transform Infrared Spectroscopy (FTIR) of (PMMA-PVA)/CuO Nanocomposite Thin Films

We employ (FTIR) technique to explore the vibrational bands of (PMMA-PVA)/CuO nanocomposites. The positions of the peaks of the FTIR patterns are found to shift due to the incorporation of CuO-NPs into (PMMA-PVA) polymeric thin films. Figure 3.31 shows FTIR spectra of (PMMA-PVA)/CuO nanocomposite thin films with (wt. % = 0%, 2%, 4%, 8%, and 16%) of CuO-NPs incorporated for a wavenumber range (500-4000) cm^{-1}. Figure 3.32(a) shows FTIR spectra of (PMMA-PVA)/CuO nanocomposite thin films for a wavenumber range (500-1500) cm^{-1}. Clearly, the FTIR spectra has three peaks at 745, 1225, and 669 cm^{-1}. The band at 669 cm^{-1} is assigned to the strong

Preprints (www.preprints.org) | NOT PEER-REVIEWED | Posted: 29 January 2021 doi:10.20944/preprints202101.0607.v1

bending stretching vibration mode of (C–O) [21]. Also, the band at 745 cm^{-1} corresponds to the vibration mode of (C–H) [21]. Furthermore, the band at 1225 cm^{-1} is associated with the strong stretch bending vibration mode of the (C–O) bond [40]. The striking observation of FTIR spectra of the as-grown thin films is the broadning and shifting to a higher wavenumber as CuO-NPs contents into (PMMA-PVA) polymeric thin films is increased. The new band of (PMMA-PVA)/CuO nanocomposite thin films is located at 1150 cm^{-1} . The band at 1150 cm^{-1} is attributed to the stretching and symmetric bending vibrationthat may be assigned to Cu–O bond [1]. Figure 3.32(b) shows FTIR spectra of (PMMA-PVA)/CuO nanocomposite thin films for a spectral range of (1500-2500) cm^{-1}. Clearly, the FTIR spectra has one peak at 1727 cm^{-1}. The broad band at 1727 cm^{-1} is attributed to the stretching modes of carbonyl (C=O) group [1, 40]. Figure 3.32(c) shows the FTIR spectra of (PMMA-PVA)/CuO nanocomposite thin films in the spectral range (2500-4000) cm^{-1}. Clearly, the FTIR spectra has two peaks at 3020 and 2952 cm^{-1}. The broad band at 3020 cm^{-1} is observed indicating the presence of the free hydroxyl (OH) groups and the stretching vibration of (C–H) [1, 35]. Furthermore, the new band at 2952 cm^{-1} is associated with the strong stretching mode of the (C–H) bond [1]. This can be interpreted in terms of the change in the strength of the bonds and the formation of new bonds that lead to the broadening and shifting of the peaks. The intensity of the peaks at 1727 and 2952 cm^{-1} are observed to decrease upon increasing CuO-NPs doping levels. The reduction of the intensities of the peaks of the entire FTIR spectra is expected and it could be attributed to the intermolecular bonding between the constituents of (PMMA-PVA)/CuO nanocomposite thin films.

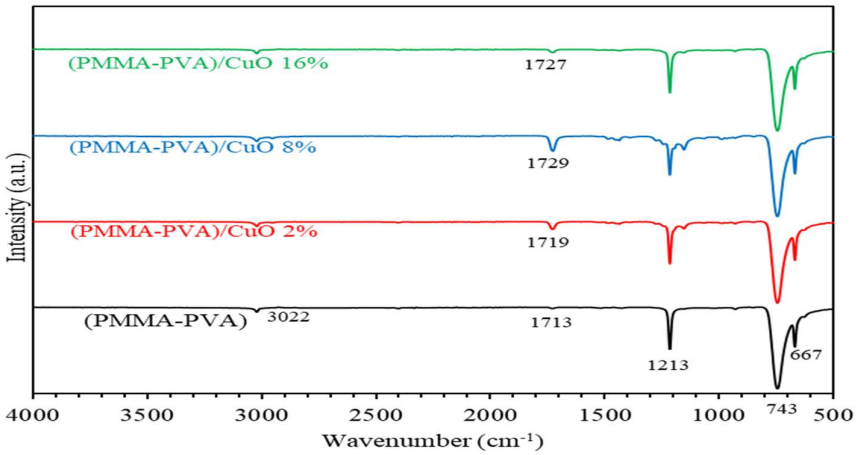

Figure 3.31. FTIR spectra of doped and un-doped for (PMMA-PVA)/CuO nanocomposite thin films.

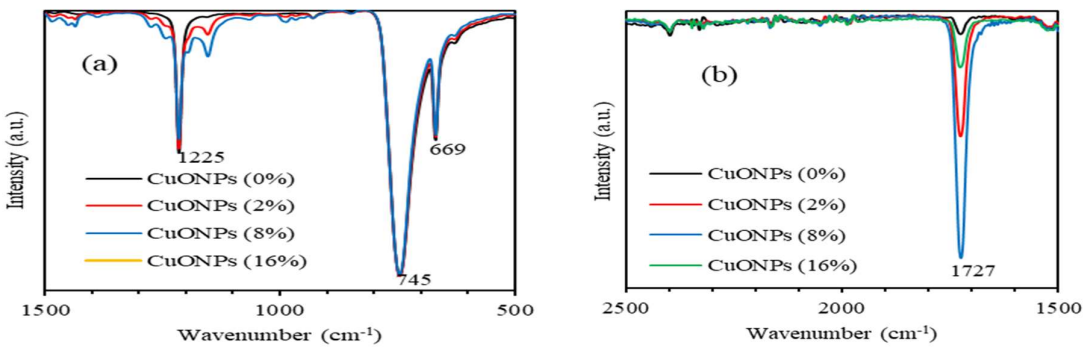

Preprints (www.preprints.org) | NOT PEER-REVIEWED | Posted: 29 January 2021 doi:10.20944/preprints202101.0607.v1

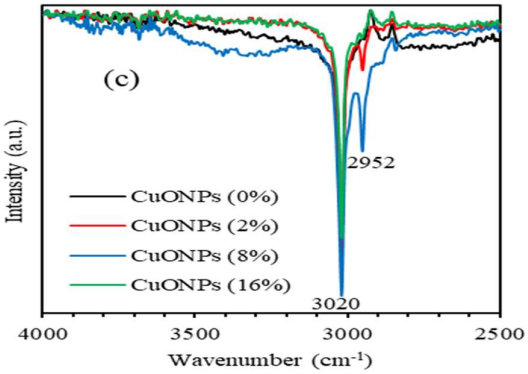

Figure 13. FTIR spectra of (PMMA-PVA)/CuO nanocomposite thin films in the spectral range (a): (500–1500cm^{-1}), (b) (1500–2500cm^{-1}) and (c): (2500–4000cm^{-1}).

3.2.2 The FTIR spectra of (PMMA-PVA) Polymeric Thin Films

Figure 5.16 shows FTIR spectra of (PMMA-PVA) polymeric thin films as a function of wavenumber in the range (500-4000) cm^{-1}. Figure 5.17 shows FTIR spectra of (PMMA-PVA) polymeric thin films in the ranges (500-1500) and (1500-2500) cm^{-1}. Our results indicate that vibrational frequencies of (PMMA-PVA) polymeric thin films coincide with several vibrational frequencies observed for pure PVA polymer thin films. This observation is attributed to the fact that PVA thin film has dense molecular packing in the polymeric nanocomposite and stronger intermolecular hydrogen bonds in comparison with the PMMA component. The weak intermolecular hydrogen bonds of PMMA is responsible for the disappearance of functional groups of PMMA in the polymer blend [41]. Furthermore, the obtained FTIR spectrum demonstrates shifts of some band positions and changes in the intensities of some other bands compared with pure PMMA and PVA polymeric thin films. These shifts and the increases of intensities of some bands are due to the strong intramolecular interactions in (PVA-PMMA) blends. For (PMMA-PVA) polymer film, vibrational band at 667 cm^{-1} could be ascribed to the (C–O) bending vibration. Whereas, the vibrational band located at 743 cm^{-1} could be attributed to the bending vibration mode of (C–H) bond. Additionally, the vibrational band positioned at 1213 cm^{-1} may be credited to the (C–O) bond stretching. Moreover, vibrational bands at 1713 cm^{-1} could be assigned to the stretching modes of carbonyl (C=O) groups [41]. Lastly, The broad band at 3020 cm^{-1} is indicating the presence of the (C–H) stretching vibration. The increase and decrease of the peak intensities of the whole FTIR spectra of (PMMA-PVA) polymeric thin films is mainly due to the intermolecular bonding between the PMMA and PVA.

Preprints (www.preprints.org) | NOT PEER-REVIEWED | Posted: 29 January 2021 doi:10.20944/preprints202101.0607.v1

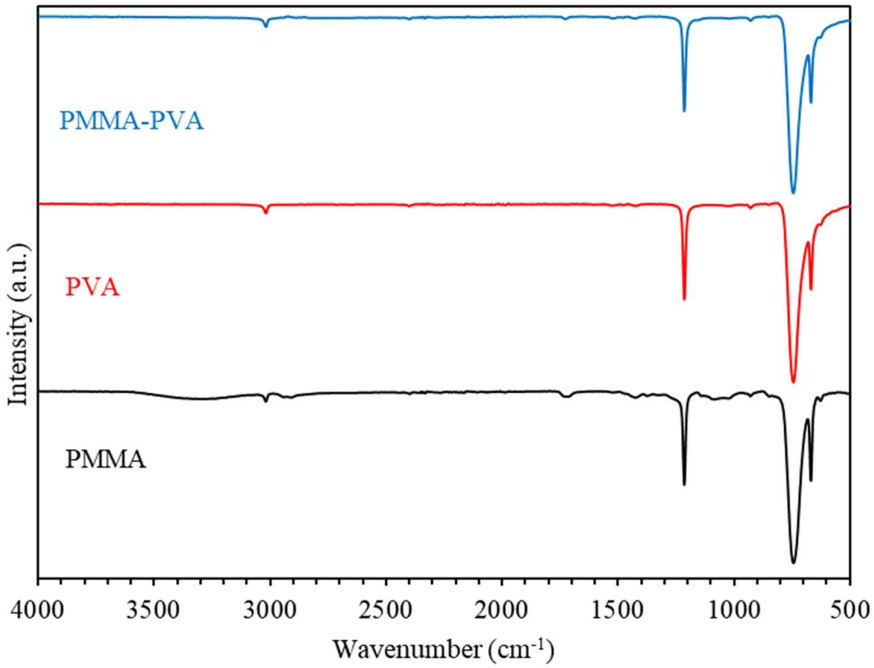

Figure 3.16. FTIR spectra of (PMMA-PVA) polymeric thin films as a function of wavenumber.

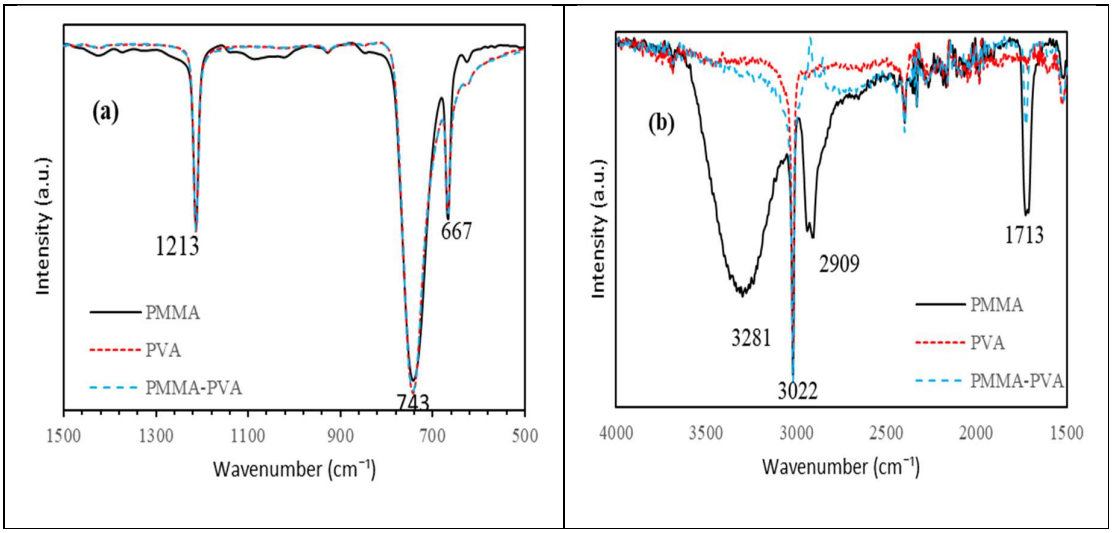

Figure 3.17. FTIR spectra of (PMMA-PVA) polymeric thin films in the spectral range (a): (500–1500cm^{-1}) and (b): (1500–4000cm^{-1}).

3.4 Thermogravimetric Analysis (TGA) of (PMMA-PVA)/CuO Nanocomposite Thin Films

The (PMMA-PVA)/CuO nanocomposite thin films thermal stability is investigated by employing thermogravimetric (TGA) analysis for temperatures up to 400 ℃. Figure 3.30 shows TGA thermograms of (PMMA-PVA)/CuO nanocomposite thin films with different concentrations of CuO-NPs. TGA thermograms of (PMMA-PVA)/CuO nanocomposite thin films show considerable weight loss (WL) steps at different temperatures. The TGA thermograms of (PMMAPVA)/CuO

Preprints (www.preprints.org) | NOT PEER-REVIEWED | Posted: 29 January 2021 doi:10.20944/preprints202101.0607.v1

nanocomposite thin films have two WL steps at 110 and 250 $°C$ regardless of the degree of incorporation of CuO-NPs. First and second WL are insignificantly shifted toward lower and higher temperatures indicating the influence of the change of intermolecular/intramolecular bonding. Clearly, the weight loss of pure (PMMA-PVA) polymeric thin films is observed to be about 92% at 400 $°C$. This value decreases as CuO-NPs content in the polymeric matrix is increased. It attains a minimum value of 45% as CuO-NPs concentration in the polymeric film is increased to 16%. The WL of the nanocomposite is inversely proportional to their wt.% of CuO-NPs content. This is a strong sign of the strengthening of physicochemical bonding density upon increasing the incorporation degree of CuO-NPs in polymeric thin films. Conveniently, (PMMAPVA)/CuO nanocomposite thin films are found to be thermally stable at temperatures below 110 $°C$. Most of the optical applications can be performed below this temperature in spite of the slight and negligible slope in the TGA thermograms below 110 $°C$ which is mostly due to water/solvent adsorption and can be easily tackled. The as-grown thin films have large photo-thermal conversion performance as employed in solar energy storage [21].

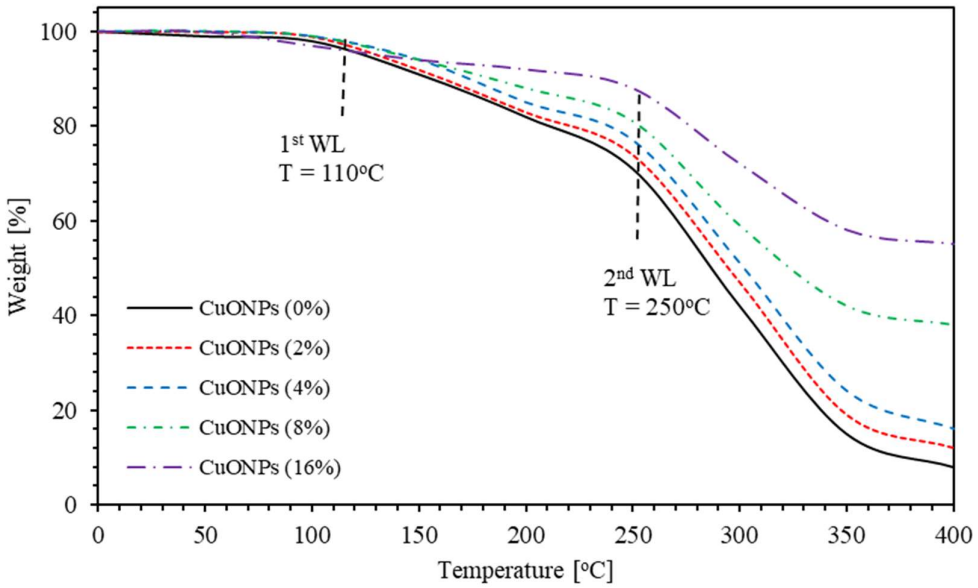

Figure 4.22. TGA curves of (PMMA-PVA)/CuO nanocomposite thin films for various CuO-NPs concentrations.

3.5 Scanning Electron Microscope (SEM)

The surface morphology of thin films is inspected using Scanning Electron Microscopy (SEM). Surface morphology of (PMMA-PVA)/CuO nanocomposite thin films at different concentrations of CuO NPs at 5 µm magnification are presented in Figure 16. Figure 16-a shows that the nanocomposite thin films of PMMA-PVA exhibit an amorphous nature with a smooth surface. Figures 16(b-e) show the CuO NPs on the surface immersed into the thin film matrix. The observed CuO NPs dimension is within the average particle size between (100–500) nm in diameter. Furthermore, SEM was used to examine the morphology and dispersion of CuO NPs on the surface of PMMA-PVA films. The SEM images show a good dispersion of CuO NPs on the surface of the PMMA-PVA films. This provides substantial evidence of the validity of our synthesis process of obtaining CuO NPs.

Preprints (www.preprints.org) | NOT PEER-REVIEWED | Posted: 29 January 2021 doi:10.20944/preprints202101.0607.v1

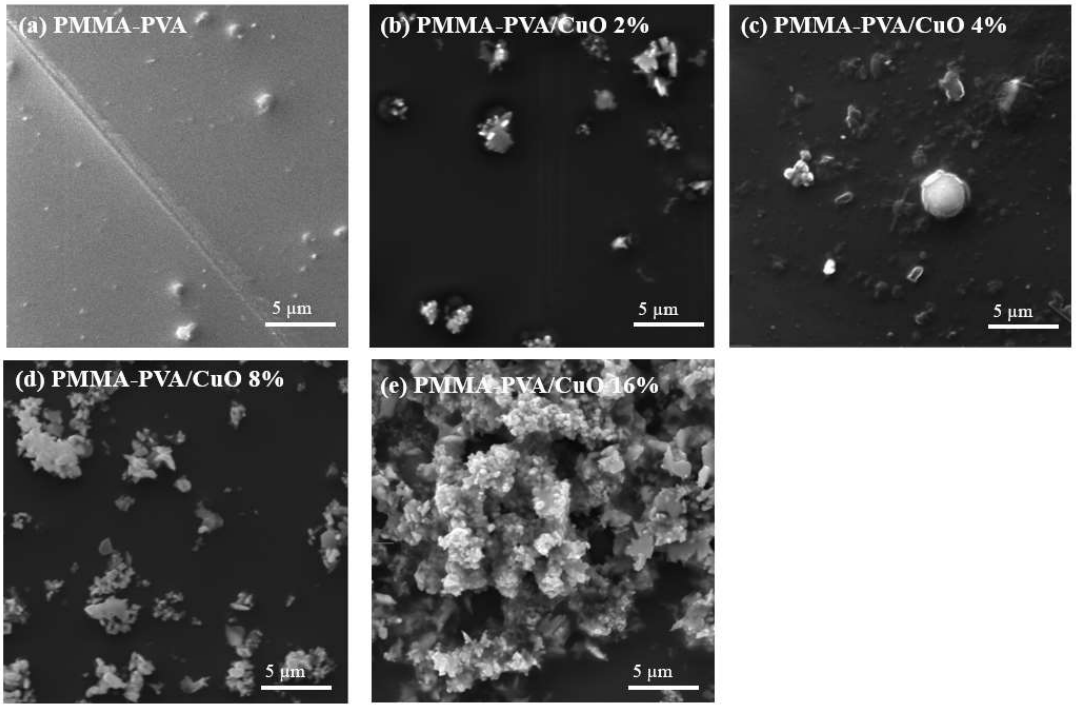

Figure 16. The SEM micrographs of (PMMA-PVA)/CuO NPs nanocomposite thin films at different concentration of CuO NPs.

5. Conclusion

In summary, (PMMA-PVA)/ CuO nanocomposite thin films with different CuO-NPs content in the range (0% to 16%) are synthesized on glass substrates using dip coating technique. Optical properties of the synthesized nanocomposite thin films including transmittance($T\%$), reflectance ($R\%$), absorption coefficient (α), optical constants (n and k) and optical dielectric functions (ε_1 and ε_2) are calculated and interpreted using experimental transmittance and reflectance spectra. Moreover, a combination of classical models such as Tauc, Urbach, Spitzer-Fan and Drude models are applied to deduce the optical, optoelectronic parameters, and the energy gaps of the prepared nanocomposite thin films. Calculated refractive indices (n) of undoped (PMMA-PVA) film is found to lie in the range (1.5 -1.85). The optical band gap of (PMMA-PVA) polymeric thin film is found to be 4.101 eV. This value decreases as CuO-NPs is introduced into polymer thin films. The obtained high refractive index values of nanocomposite thin films indicate their potential for strong optical confinement applications and enhance the optical intensities of nonlinear interactions. The high transmittance, wide band gap energy and high refractive index of the nanocomposite films indicate that doped polymerized thin films could be potential candidates for optoelectronic devices. The FTIR transmittance spectra of as-grown thin films are studied and interpreted in the spectral range (500 - 4000 cm^{-1}). Investingating thermal stability is very important. The TGA thermograms of as-prepared doped polymerized thin films show that weight loss of the nanocomposite is inveresly proportional to the wt.% of CuO-NPs. This confirms that physicochemical bonding density is strengethed by incorporating high concentration of CuO-NPs. Expediently, (PMMAPVA)/CuO thin films are thermally stable at temperatures below $110°C$. Interestingly, vast majority of optical applications operate below $110C°$. Such detailed investigation of organic-inorganic hybrid polymerized thin films would lead to the fabrication of optimized functionality.

Preprints (www.preprints.org) | NOT PEER-REVIEWED | Posted: 29 January 2021 doi:10.20944/preprints202101.0607.v1

References

[1] M. Q. Al-Gunaid, A. M. Saeed, N. K. Subramani, and B. Madhukar, "Optical parameters, electrical permittivity and I–V characteristics of PVA/Cs 2 CuO 2 nanocomposite films for opto-electronic applications," *Journal of Materials Science: Materials in Electronics,* vol. 28, no. 11, pp. 8074-8086, 2017.

[2] P. Tao *et al.*, "TiO 2 nanocomposites with high refractive index and transparency," *Journal of Materials Chemistry,* vol. 21, no. 46, pp. 18623-18629, 2011.

[3] J.-g. Liu and M. Ueda, "High refractive index polymers: fundamental research and practical applications," *Journal of Materials Chemistry,* vol. 19, no. 47, pp. 8907-8919, 2009.

[4] S. Maeda, M. Fujita, N. Idota, K. Matsukawa, and Y. Sugahara, "Preparation of transparent bulk TiO2/PMMA hybrids with improved refractive indices via an in situ polymerization process using TiO2 nanoparticles bearing PMMA chains grown by surface-initiated atom transfer radical polymerization," *ACS applied materials & interfaces,* vol. 8, no. 50, pp. 34762-34769, 2016.

[5] D. W. Mosley *et al.*, "High performance encapsulants for ultra high-brightness LEDs," in *Light-Emitting Diodes: Research, Manufacturing, and Applications XII*, 2008, vol. 6910, p. 691017: International Society for Optics and Photonics.

[6] T. Nakamura, H. Fujii, N. Juni, and N. Tsutsumi, "Enhanced coupling of light from organic electroluminescent device using diffusive particle dispersed high refractive index resin substrate," *Optical review,* vol. 13, no. 2, pp. 104-110, 2006.

[7] K. C. Krogman, T. Druffel, and M. K. Sunkara, "Anti-reflective optical coatings incorporating nanoparticles," *Nanotechnology,* vol. 16, no. 7, p. S338, 2005.

[8] J. L. Regolini, D. Benoit, and P. Morin, "Passivation issues in active pixel CMOS image sensors," *Microelectronics Reliability,* vol. 47, no. 4-5, pp. 739-742, 2007.

[9] R. Etefagh, S. Rozati, E. Azhir, N. Shahtahmasebi, and A. Hosseini, "Synthesis and antimicrobial properties of ZnO/PVA, CuO/PVA, and TiO2/PVA nanocomposites," *Scientia Iranica,* vol. 24, no. 3, pp. 1717-1723, 2017.

[10] C. DeMerlis and D. Schoneker, "Review of the oral toxicity of polyvinyl alcohol (PVA)," *Food and chemical Toxicology,* vol. 41, no. 3, pp. 319-326, 2003.

[11] A. Almusawe, R. Kadhum, T. Hassen, and N. Abd Alrasheed, "Study of Gamma Irradiation Effect on the Optical Properties of Bromocresol Green Dye Doped Poly Methyl Methacrylate Thin Films," *Results Phys.,* vol. 7, pp. 807-809, 2017.

[12] M. M. Demir, M. Memesa, P. Castignolles, and G. Wegner, "PMMA/zinc oxide nanocomposites prepared by in-situ bulk polymerization," *Macromolecular Rapid Communications,* vol. 27, no. 10, pp. 763-770, 2006.

[13] A. El Sayed, S. El-Gamal, W. Morsi, and G. Mohammed, "Effect of PVA and copper oxide nanoparticles on the structural, optical, and electrical properties of carboxymethyl cellulose films," *Journal of Materials Science,* vol. 50, no. 13, pp. 4717-4728, 2015.

[14] V. Patake, S. Joshi, C. Lokhande, and O.-S. Joo, "Electrodeposited porous and amorphous copper oxide film for application in supercapacitor," *Materials Chemistry and Physics,* vol. 114, no. 1, pp. 6-9, 2009.

[15] G. Ren, D. Hu, E. W. Cheng, M. A. Vargas-Reus, P. Reip, and R. P. Allaker, "Characterisation of copper oxide nanoparticles for antimicrobial applications," *International journal of antimicrobial agents,* vol. 33, no. 6, pp. 587-590, 2009.

[16] S. Shariffudin, S. Khalid, N. Sahat, M. Sarah, and H. Hashim, "Preparation and characterization of nanostructured CuO thin films using sol-gel dip coating," in *IOP*

Preprints (www.preprints.org) | NOT PEER-REVIEWED | Posted: 29 January 2021 doi:10.20944/preprints202101.0607.v1

Conference Series: Materials Science and Engineering, 2015, vol. 99, no. 1, p. 012007: IOP Publishing.

[17] R. Sonawane, S. Hegde, and M. Dongare, "Preparation of titanium (IV) oxide thin film photocatalyst by sol–gel dip coating," *Materials chemistry and physics,* vol. 77, no. 3, pp. 744-750, 2003.

[18] A. Y. Fasasi *et al.*, "Effect of Precursor Solvents on the Optical Properties of Copper Oxide Thin Films Deposited Using Spray Pyrolysis for Optoelectronic Applications," *American Journal of Materials Synthesis and Processing,* vol. 3, no. 2, pp. 12-22, 2018.

[19] A. Moumen, B. Hartiti, E. Comini, H. M. M. Arachchige, S. Fadili, and P. Thevenin, "Preparation and characterization of nanostructured CuO thin films using spray pyrolysis technique," *Superlattices and Microstructures,* vol. 127, pp. 2-10, 2019.

[20] G. D. D. P. M. Methacrylate, "Study of Gamma irradiation effect on the Optical Properties of Bromocresol Green Dye Doped Poly Methyl Methacrylate Thin Films."

[21] B. Xu, J. Zhou, Z. Ni, C. Zhang, and C. Lu, "Synthesis of novel microencapsulated phase change materials with copper and copper oxide for solar energy storage and photo-thermal conversion," *Solar Energy Materials and Solar Cells,* vol. 179, pp. 87-94, 2018.

[22] S. Elmaghrum, R. Copperwhite, B. Corcoran, C. McDonagh, and A. Gorin, "Optical Properties Of High Refractive Index Thin Films Processed At Low-Temperature," 2012.

[23] M. Oubaha, S. Elmaghrum, R. Copperwhite, B. Corcoran, C. McDonagh, and A. Gorin, "Optical properties of high refractive index thin films processed at low-temperature," *Optical Materials,* vol. 34, no. 8, pp. 1366-1370, 2012.

[24] D. Stuerga, "Microwave-material interactions and dielectric properties, key ingredients for mastery of chemical microwave processes," *Microwaves in organic synthesis,* vol. 2, pp. 1-59, 2006.

[25] A. Ahmad, A. Alsaad, Q. Al-Bataineh, and M. Al-Naafa, "Optical and structural investigations of dip-synthesized boron-doped ZnO-seeded platforms for ZnO nanostructures," *Applied Physics A,* vol. 124, no. 6, p. 458, 2018.

[26] C. Kittel, "Introduction to Solid State Physics, 6th edn., translated by Y," *Uno, N. Tsuya, A. Morita and J. Yamashita,(Maruzen, Tokyo, 1986) pp,* pp. 124-129, 1986.

[27] Z. C. Jin, I. Hamberg, and C. Granqvist, "Optical properties of sputter-deposited ZnO: Al thin films," *Journal of applied physics,* vol. 64, no. 10, pp. 5117-5131, 1988.

[28] A. S. Hassanien, "Studies on dielectric properties, opto-electrical parameters and electronic polarizability of thermally evaporated amorphous Cd50S50− xSex thin films," *Journal of Alloys and Compounds,* vol. 671, pp. 566-578, 2016.

[29] B. Mol *et al.*, "Radio frequency plasma polymerized thin film based on eucalyptus oil as low dielectric permittivity, visible and near-infrared (NIR) photoluminescent material," *Journal of Materials Science: Materials in Electronics,* vol. 30, no. 13, pp. 12603-12611, 2019.

[30] J. Tauc, *Amorphous and liquid semiconductors*. Springer Science & Business Media, 2012.

[31] M. El-Hagary, M. Emam-Ismail, E. Shaaban, and A. El-Taher, "Effect of γ-irradiation exposure on optical properties of chalcogenide glasses Se70S30− xSbx thin films," *Radiation Physics and Chemistry,* vol. 81, no. 10, pp. 1572-1577, 2012.

[32] F. Urbach, "The long-wavelength edge of photographic sensitivity and of the electronic absorption of solids," *Physical Review,* vol. 92, no. 5, p. 1324, 1953.

Preprints (www.preprints.org) | NOT PEER-REVIEWED | Posted: 29 January 2021 doi:10.20944/preprints202101.0607.v1

[33] R. Parmar, R. Kundu, R. Punia, P. Aghamkar, and N. Kishore, "Iron modified structural and optical spectral properties of bismuth silicate glasses," *Physica B: Condensed Matter,* vol. 450, pp. 39-44, 2014.

[34] H. Chamroukhi *et al.*, "Optical and structural properties enhancement of hybrid nanocomposites thin films based on polyaniline doped with Zinc Oxide embedded in bimodal mesoporous silica (ZnO@ SiOX) nanoparticles," *Optical Materials,* vol. 84, pp. 703-713, 2018.

[35] N. Dhineshbabu, V. Rajendran, N. Nithyavathy, and R. Vetumperumal, "Study of structural and optical properties of cupric oxide nanoparticles," *Applied Nanoscience,* vol. 6, no. 6, pp. 933-939, 2016.

[36] A. Fasasi *et al.*, "Effect of Precursor Solvents on the Optical Properties of Copper Oxide Thin Films Deposited Using Spray Pyrolysis for Optoelectronic Applications," *Amer. J. Mater. Synth. Process,* vol. 3, pp. 12-22, 2018.

[37] W. Spitzer and H. Fan, "Determination of optical constants and carrier effective mass of semiconductors," *Physical Review,* vol. 106, no. 5, p. 882, 1957.

[38] A. Farag, A. Ashery, and M. Shenashen, "Optical absorption and spectrophotometric studies on the optical constants and dielectric of poly (o-toluidine)(POT) films grown by spin coating deposition," *Physica B: Condensed Matter,* vol. 407, no. 13, pp. 2404-2411, 2012.

[39] Z. Ibupoto, K. Khun, V. Beni, X. Liu, and M. Willander, "Synthesis of novel CuO nanosheets and their non-enzymatic glucose sensing applications," *Sensors,* vol. 13, no. 6, pp. 7926-7938, 2013.

[40] S. Rajagopal, *The Forensic Analysis of Skin-Safe Stamp Pad Inks*. John Jay College of Criminal Justice, 2019.

[41] S. Kaur and K. S. Samra, "Study of optical and structural properties of PVA/PMMA blend," Lovely Professional University, 2017.